RSC Advances

PAPER

View Article Online
View Journal | View Issue

Cite this: *RSC Adv.*, 2014, **4**, 17805

Removal of Cr(VI) from water using polypyrrole/attapulgite core–shell nanocomposites: equilibrium, thermodynamics and kinetics

Yong Chen,* Hui Xu, Shiyu Wang and Long Kang

Received 9th December 2013
Accepted 1st April 2014

DOI: 10.1039/c3ra47351a

www.rsc.org/advances

In this study polypyrrole (PPy) was synthesised chemically on the surface of attapulgite (ATP) to form nanocomposites using ATP as nucleus and PPy as shell. Transmission electron microscopy (TEM) and scanning electron microscopy (SEM) showed that ATP was coated with a PPy layer. PPy/ATP nanocomposites as adsorbents were used to remove Cr(VI) from aqueous solutions. External factors were investigated, including contact time, adsorbent dose, initial concentration of adsorbate and pH. The experimental data are well fitted with the Langmuir isotherm model. The thermodynamic parameters were evaluated and the results revealed that the adsorption process was exothermic and spontaneous. The kinetic data indicated that the adsorption process followed a pseudo-second-order equation, implying that the adsorption process was predominantly controlled by chemical processes. The associated adsorption mechanism for Cr(VI) removal by the PPy/ATP nanocomposites was investigated using X-ray photoelectron spectroscopy (XPS), which suggests that ion change and reduction processes on the surface of the nanocomposites may be the possible mechanism.

1. Introduction

The removal of toxic heavy metals from environmental water resources introduced by industrial pollution is considered to be a global environmental issue. Chromium is one of the heavy metals and its compounds are extensively used in chemical industries such as electroplating, textile, leather tanning, metal finishing, wood preservation, electroplating and chromate preparation industries.[1,2] Chromium is most commonly found in two oxidation states, Cr(III) and Cr(VI), and other oxidation states are not stable in aerated aqueous media.[2] Among them Cr(VI) is highly poisonous and endangers public health. However, different from Cr(III), which can be easily adsorbed onto all kinds of inorganic and organic materials at neutral pH, Cr(VI) is only weakly adsorbed onto inorganic surfaces.[3] Thus, how to remove Cr(VI) from wastewater utilizing efficient method is considered to be of urgency.

During recent years, various treatment processes have been employed to remove Cr(VI) from water, for example, adsorption, chemical treatment, ion exchange, electrochemical reduction and membrane separation.[4] Among these methods, adsorption is extensively used because of the feasibility and low cost. However, most of adsorbents, such as activated carbon, zeolite and silicone have some flaws, for instance, excessive time requirements, high costs and inefficiency. Therefore, it is urgent to explore a highly efficient adsorbent.

College of Perochemical Engineering, Lanzhou University of Technology, Lanzhou 730050, P.R. China. E-mail: yongchen2003@126.com; Tel: +86 931 2973560

Since their discovery three decades ago, conducting polymers have attracted more and more attention and a lot of research work has been done to probe into their physical and chemical properties.[5] PPy, as one of the conducting polymers, has been widely applied in various fields due to its good electrical, electrochemical properties, environmental stability to water and oxygen, and ease of preparation at low cost.[6] These applications mainly focus on its interesting electrical conductivity. However, some studies have found that PPy synthesized in solutions with small or large dopants mainly exhibits anion-exchanger or cation-exchanger behavior.[7–9] Thus, due to its excellent property of ion exchange, PPy can be used as an adsorbent to remove heavy metal ions from aqueous solution.

ATP, a kind of crystalline hydrated magnesium aluminum silicate mineral with large surface area, excellent chemical stability and strong adsorption,[10,11] has been intensively utilized as adsorbent for the removal of heavy metal ions. However, ATP may easily agglomerate due to its large surface area, and therefore its adsorption efficiency becomes low. To overcome these disadvantages, various methods were applied to improve the adsorption efficiency of ATP. One of methods is modification,[12] and after modified, ATP can successfully improve its adsorption capabilities.

In this work, PPy prepared with chloride ion as a dopant was employed to modify ATP to form nanocomposites and the composites were exploited to remove Cr(VI) from aqueous water. The batch sorption method was used to investigate adsorption equilibrium, kinetics and thermodynamics of the adsorption process.

2. Experiment

2.1 Materials

Pyrrole was purchased from Shanghai Zhongqin Chemical Reagent Co. Ltd. and was distilled prior to use. ATP was supplied by Jiangsu Xuyi. Anhydrous ferric chloride ($FeCl_3$), as oxidant and dopant for polymerization of pyrrole and potassium dichromate ($K_2Cr_2O_7$), were purchased from Yantai Shuangshuang chemical Co. Ltd. Stock solution of Cr(VI) was prepared by dissolving $K_2Cr_2O_7$ in distilled water. All other reagents used were of analytical-reagent grade.

2.2 The preparation of nanocomposites

5 g $FeCl_3$ was added into 100 mL distilled water and stirred until totally dissolved. 1 g ATP was added into the solution, then freshly distilled pyrrole was dropwise added into the mixture and black precipitation appeared. The reaction was allowed to continue for 4 h, then the precipitation was filtered, washed with distilled water and acetone until the washing liquid was colorless, and dried at temperature about 60 °C for 4 h.

2.3 Adsorption experiments

A certain concentration of Cr(VI) (100 mL) and adsorbent (PPy/ATP nanocomposites) were added into a flask. After stirring for a certain time, the suspension liquid was filtered. A spectrophotometer was employed for analysis of Cr(VI) in the filtrate. The removal efficiency of Cr(VI) (%) and the adsorption capacity q_t (mg g^{-1}) were calculated by eqn (1) and (2).

$$\text{Removal efficiency } (\%) = \frac{c_0 - c_t}{c_0} \times 100\% \quad (1)$$

$$q_t = \frac{(c_0 - c_t) \times V}{m} \quad (2)$$

where c_0 is the initial concentration (mg L^{-1}) and c_t is the final concentration (mg L^{-1}). V was the solution volume (mL) and m was the mass of PPy/ATP adsorbent (g).

2.4 Instrument of characterization

FT-IR spectra measurements were done on a Spectrum 100 spectrometer (Perkin Elmer, USA) using the KBr pellets. The morphology of nanocomposites was examined using a JSM-670 scanning electron microscope (SEM) (Electronics optical Ltd., Japan). Transmission electron microscopy (TEM) was taken by using a JEM-1200EX transmission electron microscopy operated at 200 kV (FEI, USA). XPS data of PPy/ATP nanocomposites were obtained using an ESCALAB 210 Instrument. A Spectrophotometer (Shanghai Scientific Instrument Corporation, 7230G) was employed for analysis of Cr(VI).

3. Results and discussion

3.1 Characterization of PPy/ATP nanocomposites

The FTIR spectra of ATP, PPy, PPy/ATP nanocomposites (before adsorption and after adsorption) are respectively shown in Fig. 1. It can be seen from Fig. 1(a) that the characteristic peaks at 3563 cm^{-1} and 3417 cm^{-1} correspond to –OH stretching vibration causing by mineral layer and surface adsorbed water and the peak at 1655 cm^{-1} corresponds to –OH stretching vibration of H_2O. In addition, the peaks at 1032 cm^{-1} and 793 cm^{-1}, 472 cm^{-1} are respectively attributed to Si–O–Si stretching vibration and bending vibration.[13] In Fig. 1(b) the peak at 3430 cm^{-1} is assigned to the N–H stretching vibrations.[9] The peak at 1630 cm^{-1} is attributed to the conjugate molecular structure of PPy and the free charge carrier present in the polymer.[14] The band at 1535 cm^{-1} corresponds to C=C stretching vibration and the band at 1160 cm^{-1} reflects C–N stretching vibration. The bands of the C–H in-plane stretching vibration and out-plane bending vibration are situated at 1030 cm^{-1} and 772 cm^{-1}.[6] The spectrum of PPy/ATP nanocomposites (before adsorption) (Fig. 1(c)) clearly exhibits characteristic absorption peaks with respect to PPy (Fig. 1(b)), which indicates the formation of PPy in nanocomposites. Also, there is no difference between Fig. 1(c) and (d), which implies that no new species generated after adsorption.

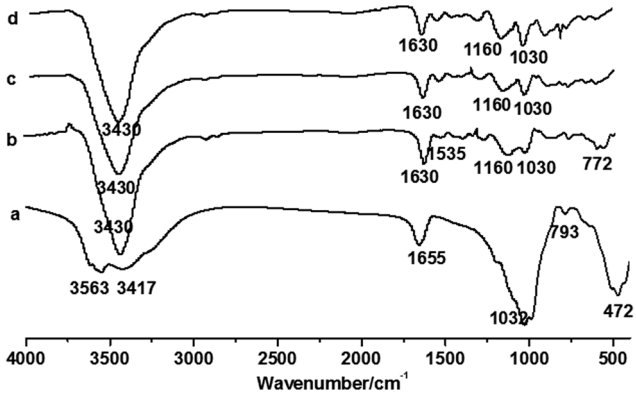

Fig. 1 FTIR spectra of (a) attapulgite (b) polypyrrole (c) PPy/ATP nanocomposites before adsorption (d) PPy/ATP nanocomposites after adsorption.

The morphology of ATP and PPy/ATP nanocomposites is illustrated in Fig. 2. As can be seen from Fig. 2(a) and (b) that ATP without any modification is rod-like structure but poor dispersion. Fig. 2(c) and (d) respectively have the same magnification factor with (a) and (b). Compared with Fig. 2(a), many holes can be observed in Fig. 2(c), which means that the structure of nanocomposites is loose and has good dispersion. With the magnification improvement, high dispersion rod-like structure can be seen from Fig. 2(d) and it is clearly observed that some PPy microspheres coat the surface of ATP. The result is further proved by TEM image of nanocomposites. Fig. 2(e) shows that the surface of the PPy/ATP nanocomposites is rougher and covered by PPy layer. The analysis demonstrates that rod-like nanocomposites can be formed employing ATP as nucleus and PPy as shell.

3.2 Effect of contact time

Fig. 3 shows the effect of contact time on adsorption of Cr(VI) by PPy/ATP nanocomposites. For these cases, initial concentration of Cr(VI) was of 100 mg L^{-1}, PPy/ATP dose of 0.1 g were used and temperature was 298 K. When contact time is 30 s, the removal efficiency of Cr(VI) reaches up to 95.21%, which indicates that

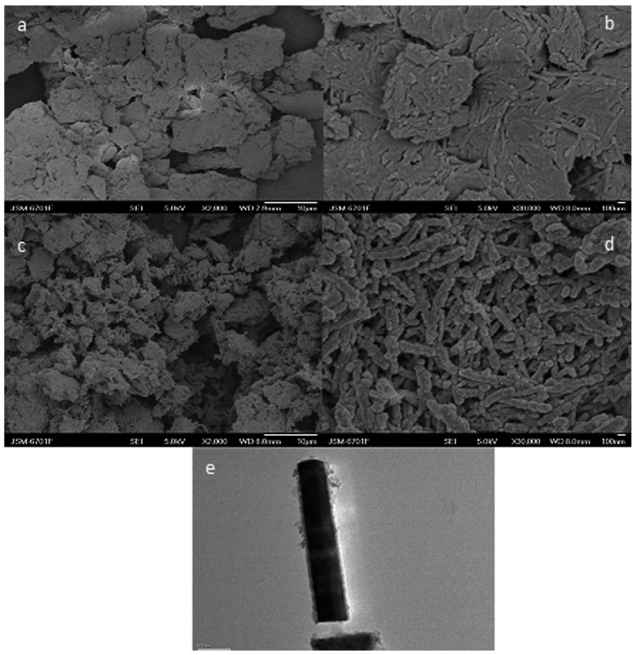

Fig. 2 SEM micrographs of (a) & (b) attapulgite, (c) & (d) PPy/ATP nanocomposites, TEM image of (e) PPy/ATP nanocomposites.

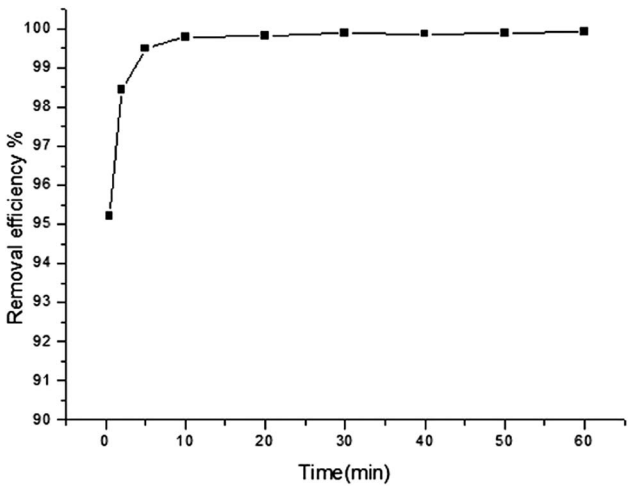

Fig. 3 Effect of time on adsorption of Cr(VI).

most of Cr(VI) can be removed during such a short time. When contact time is 10 min, the removal efficiency reaches up to 99.79%, and then little change of removal efficiency is observed. This may be due to the fact that once a certain number of Cr(VI) is removed by quantitative adsorbent within a given time, no more adsorption occurs afterwards. The results demonstrate that it is sufficient for removing Cr(VI) from water by PPy/ATP with a very minimum contact time. Based on these results, a contact time of 10 min was chosen for further experiment.

3.3 Effect of adsorbent dose

The effect of adsorbent dose on Cr(VI) removal was studied at 298 K and at initial Cr(VI) concentration of 100 mg L^{-1} by allowing a contact time of 10 min. The results are depicted in Fig. 4. It can be clearly seen from Fig. 4 that the adsorption capacity reduces and removal efficiency increases with improvement of adsorbent dose. When adsorbent dose reaches to 0.2 g, the adsorption capacity becomes 46.14 mg g^{-1} and the removal efficiency of Cr(VI) reaches up to 92.27%. Considering two factors (adsorption capacity and removal efficiency), further experiments were carried out with adsorbent dose of 0.2 g.

3.4 Effect of initial concentration of Cr(VI)

The initial concentration of 10, 25, 40, 50, 65, 85, 100 mg L^{-1} of Cr(VI) at 10 min contact time and 0.2 g dose was investigated. As shown in Fig. 5, the removal efficiency of Cr(VI) decreases with increasing of initial Cr(VI) concentration. When the initial concentration of Cr(VI) is less than 50 mg L^{-1}, the removal efficiency (99%) is almost unchanged. However, When the initial concentration of Cr(VI) is more than 50 mg L^{-1}, the removal efficiency is lower than 99%. At low concentration the removal efficiency is higher due to a larger surface area of PPy/ATP nanocomposites being available for the adsorption of

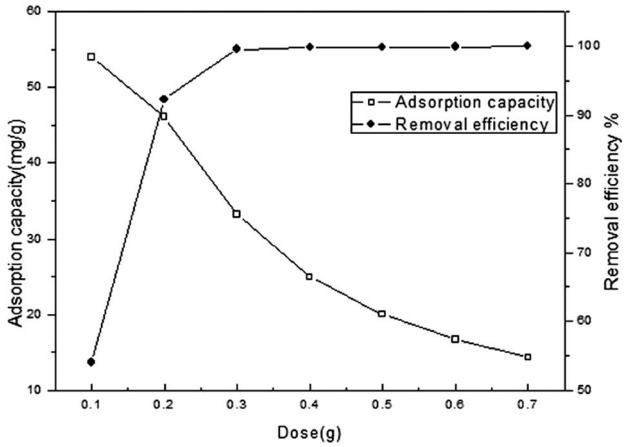

Fig. 4 Effect of adsorbent dose on adsorption of Cr(VI).

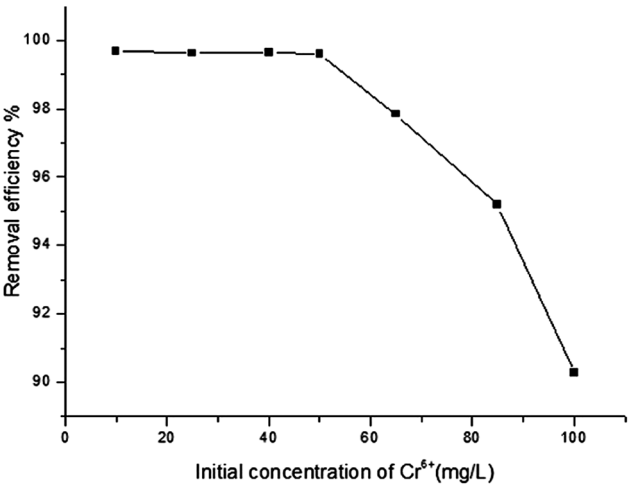

Fig. 5 Effect of initial concentration of Cr(VI) on adsorption.

Cr(VI). When the initial concentration of Cr(VI) becomes higher, the removal efficiency will be lower, because the available sites of adsorption will become less with the initial amount of Cr(VI) increasing. Another reason is the oxidative nature of Cr(VI), high concentration of Cr(VI) may damage the PPy structure, which leads to the decrease of the removal efficiency.[1]

3.5 Effect of pH

The chemistry of Cr(VI) in aqueous solution is very pH dependent. In the range of pH 2.0–6.0, the predominant Cr(VI) species are monovalent bichromate ($HCrO_4^-$) and dichromate ($Cr_2O_7^{2-}$), and when the pH value is above 6.0, the dominant species is (CrO_4^{2-}) ions.[1,2] So, in order to find out the optimum pH for the maximum removal efficiency of Cr(VI) the effect of pH on adsorption was examined at 298 K, 10 min contact time and 0.2 g dose. In this experiment, 100 mL of 50 mg L^{-1} Cr(VI) solution was prepared in different pH, ranging from 1.0 to 11.0 using HCl and NaOH solutions. Fig. 6 shows the results and it is clear that the removal efficiency of Cr(VI) can reach up to above 96% in acidic and weakly alkaline medium (pH = 1.0–10.0). The best pH value for Cr(VI) removal is found to be 3 (99.27%), and when the pH value is above 10.0, the removal efficiency will rapidly decline (91.18%). To remove Cr(VI) by PPy/ATP nanocomposites is mainly through the anion exchange process by replacing the doped Cl^- ions with $HCrO_4^-$, $Cr_2O_7^{2-}$ or CrO_4^{2-} in the treated solutions. When the pH values are low, the anion exchange process can be easily carried out. However, with the pH values increasing, the number of hydroxyl (OH^-) in the solution also increases, leading to the competitive interaction between CrO_4^{2-} and OH^- for the limited adsorption sites. As a result, the removal efficiency of Cr(VI) declines.

Furthermore, anion exchange is not the only mechanism of the adsorption process, and a redox reaction between Cr(VI) and electron rich polymer may also occur. For confirming the redox process X-ray photoelectron spectroscopy (XPS) was used to analyze PPy/ATP nanocomposites after adsorption. XPS spectrum is exhibited in Fig. 7. Two energy bands at 577.13 eV and 586.75 eV assigning to the banding energies of Cr (2p3/2) and Cr (2p1/2) orbital's, are observed. This observation implies the existence of both Cr(III) and Cr(VI).[2,15,16] In other words, the existence of Cr(III) on the surface of PPy/ATP nanocomposites suggests that Cr(VI) adsorbed by PPy/ATP nanocomposites is partially reduced to Cr(III) by electron rich polypyrrole moieties in the nanocomposites.

3.6 Adsorption thermodynamics

Adsorption isotherms are important for the description of how adsorbate interacts with adsorbent surface and are also critical in optimizing the use of an adsorbent. Adsorption isotherms were studied at five different temperatures with varying initial concentration of Cr(VI) from 25 to 100 mg L^{-1}. Two well known isotherm equations, *i.e.*, Langmuir and Freundlich equation, have been employed to plot the isotherms. The linearized Langmuir and Freundlich models are mathematically expressed as eqn (3) and (4).

$$\frac{c_e}{q_e} = \frac{1}{bq_m} + \frac{c_e}{q_m} \quad (3)$$

$$\ln q_e = \ln k_F + \frac{1}{n} \ln c_e \quad (4)$$

where q_m is the maximum adsorption capacity (mg g^{-1}) of the PPy/ATP nanocomposites; b is the free energy of adsorption (L mg^{-1}); k_F and n are the Freundlich isotherm parameters related to the adsorption capacity (mg g^{-1}) and the intensity of adsorption. The linearized results and calculated values of Langmuir and Freundlich constants are listed in Tables 1 and 2.

Based on the higher values of correlation coefficients (R^2), adsorption data are better described by the Langmuir model than that of Freundlich model, which indicates that the adsorption of Cr(VI) on the surface of PPy/ATP nanocomposites is a monolayer adsorption. The value of q_m decreases from 48.45 mg g^{-1} to 27.06 mg g^{-1} with improvement in temperature from

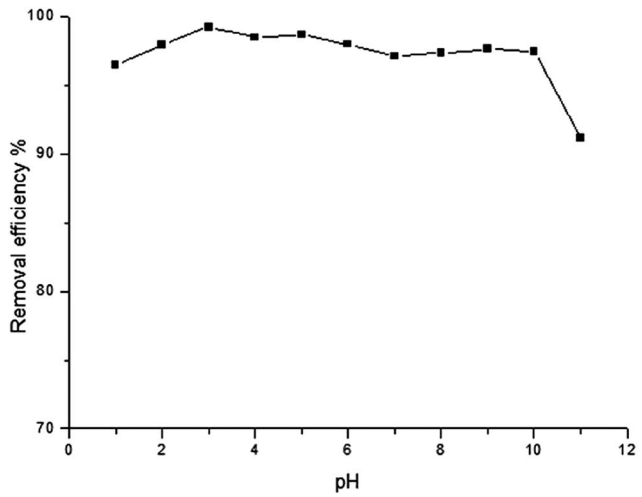

Fig. 6 Effect of pH value on adsorption of Cr(VI).

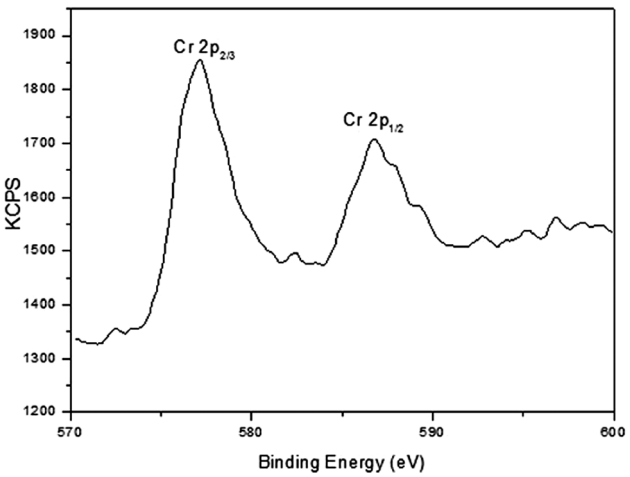

Fig. 7 XPS spectra of the PPy/ATP nanocomposites after Cr(VI) adsorption.

Table 1 Langmuir isotherms regression equation and constants for Cr(VI) adsorption onto PPy/ATP

Temperature/K	Regression equation c_e/q_e	R^2	q_m/(mg g^{-1})	b/(L mg^{-1})
298	$0.02064C_e + 0.00302$	0.99838	48.45	6.8344
303	$0.02092C_e + 0.006$	0.99841	47.8	3.4867
308	$0.03673C_e + 0.03388$	0.99756	27.23	1.0841
313	$0.03714C_e + 0.02348$	0.99825	26.93	1.5818
318	$0.03696C_e + 0.01284$	0.99565	27.06	2.8785

Table 2 Freundlich isotherms regression equation and constants for Cr(VI) adsorption onto PPy/ATP

Temperature/K	Regression equation ln q_e	R^2	K	n^{-1}
298	$3.58596 + 0.23748 \ln C_e$	0.81517	36.088	0.23748
303	$3.43702 + 0.24815 \ln C_e$	0.86026	31.094	0.24815
308	$2.76863 + 0.15732 \ln C_e$	0.82793	15.937	0.15732
313	$2.81074 + 0.14643 \ln C_e$	0.93769	16.621	0.14643
318	$2.89699 + 0.12596 \ln C_e$	0.79618	18.120	0.12596

298 K to 318 K. This reveals that the exothermic nature of the adsorption process.

3.7 Thermodynamic study

To study the thermodynamics of adsorption of Cr(VI) on PPy/ATP nanocomposites, the thermodynamic parameters such as Gibbs free energy change (ΔG), enthalpy change (ΔH) and entropy change (ΔS) were determined by using eqn (5) and (6).[17]

$$\Delta G = -RT \ln K_D \quad (5)$$

$$\ln K_D = -\frac{\Delta H}{RT} + \frac{\Delta S}{R} \quad (6)$$

where R is the ideal gas constant (8.314 J mol^{-1} K) and T is the temperature in Kelvin. The values of, ΔG, ΔH, ΔS and can be calculated from the slope and intercept of the ln K_D *versus* $1/T$. The results are listed in Table 3. The enthalpy change is negative which is consistent with the exothermic nature of the adsorption process. The negative value of Gibbs free energy change indicates the thermodynamic feasibility and the spontaneous nature of the adsorption. Meanwhile, the negative value of entropy change suggests an increase in order at the solid–liquid interface.

3.8 Kinetics of adsorption

The effect of adsorption time on the uptake of Cr(VI) at four different initial concentrations of Cr(VI) (*i.e.*, 25, 40, 50 and 65 mg L^{-1}) is depicted in Fig. 8. The adsorption capacity of Cr(VI) increases with an improvement in adsorption time until the equilibrium is established between the solid phase and liquid phase in the adsorption system at 200 s. Various kinetics models, namely pseudo-first-order kinetics, pseudo-second-order kinetics and intra-particle diffusion model have been used for their validity with the experimental adsorption data for the Cr(VI) on PPy/ATP nanocomposites. These kinetic equations can be linearly expressed as follows:

$$\ln(q_e - q_t) = \ln q_e - k_1 t \text{ (pseudo-first-order kinetics equation)}$$

$$\frac{t}{q_t} = \frac{t}{k_2 q_e^2} + \frac{t}{q_e} \text{ (pseudo-second-order kinetics equation)}$$

$$q_t = k_p t^{0.5} \text{ (intra-particle diffusion equation)}$$

where q_e and q_t are the adsorption capacity (mg g^{-1}) of the adsorbent at equilibrium and at time t (s), respectively, k_1(min^{-1}) is the pseudo-first-order rate constant, k_2 (g mg^{-1} s) is the pseudo-second-order rate constants and k_p (mg g^{-1} s^{-1}0.5) is the intra-particle diffusion rate constant. The linearizing results are shown in Table 4. According to the correlation coefficient (R^2), the kinetic data indicate that the adsorption process is controlled by pseudo-second-order model, which implies that the Cr(VI) uptake process is due to chemisorptions. The assumption behind the pseudo-second-order model is that the rate-limiting step may be chemisorptions involving valence

Table 3 Thermodynamic parameter for Cr(VI) adsorption onto PPy/ATP

Temperature/K	ΔH/(kJ mol^{-1})	ΔG/(kJ mol^{-1})	ΔS/(J mol^{-1} K^{-1})
298	−113.685	−14.376	−333.56
303	−113.685	−12.887	−333.56
308	−113.685	−10.116	−333.56
313	−113.685	−9.762	−333.56
318	−113.685	−11.514	−333.56

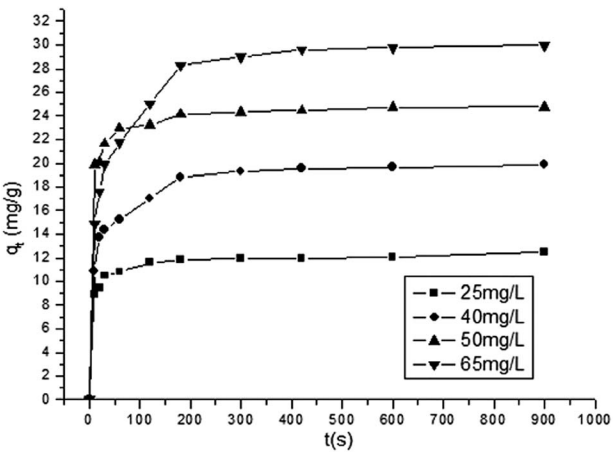

Fig. 8 Adsorption kinetic curves of (VI) onto PPy/ATP nanocomposites.

Table 4 Parameters for kinetic models of Cr(VI) adsorption onto PPy/ATP

	Pseudo-first-order kinetics		Pseudo-second-order kinetics		Intra particle diffusion model	
C_0 (mg L^{-1})	k_1/(min^{-1})	R^2	$k_2 \times 10^{-5}$/(g mg^{-1} s^{-1})	R^2	k_p/(mg g^{-1} s^{-1})	R^2
25	0.00955	0.75487	1069	0.99972	0.13132	0.70609
40	0.01124	0.95717	431	0.99982	0.38041	0.38041
50	0.00868	0.75943	750	0.99998	0.2227	0.76969
65	0.00457	0.69378	189	0.99987	0.6553	0.80751

forces through sharing or exchange of electrons between adsorbent and adsorbate.

4. Conclusions

For the first time PPy/ATP core–shell nanocomposites were successfully prepared *in situ* polymerization technique. The nanocomposites exhibited considerable potential for the removal of Cr(VI) from aqueous solution. The optimum conditions of adsorption were found to be: contact time of 10 min, an adsorbent dose of 0.2 g and Cr(VI) initial concentration of 50 mg L^{-1}. Also the removal of Cr(VI) can keep high removal efficiency under acidic or neutral conditions. The results from this experiment are well fitted with Langmuir models, and the thermodynamic research show that the adsorption process is spontaneous and exothermic. The kinetic data indicate that the adsorption process is described by pseudo-second-order equation. The mechanism for the removal of Cr(VI) by PPy/ATP nanocomposites is a combined effect of anion exchange and redox of Cr(VI) to Cr(III). The results demonstrate that PPy/ATP nanocomposites can be considered as an optimum material for the removal of Cr(VI) from aqueous solution.

Acknowledgements

This work was supported by the National Natural Science Foundation (51062011), Gansu Natural Science Youth Foundation (1208RJYA086) and the Hong Liu Youth Train Plan of Lanzhou University of Technology (Q201013).

References

1 R. Ansari and N. Khoshbakht Fahim, Application of polypyrrole coated on wood sawdust for removal of Cr(VI) ion from aqueous solutions, *React. Funct. Polym.*, 2007, **67**, 367–374.
2 M. Bhaumik, A. Maity, V. V. Srinivasu and M. S. Onyango, Enhanced removal of Cr(VI) from aqueous solution using polypyrrole/Fe_3O_4 magnetic nanocomposite, *J. Hazard. Mater.*, 2011, **190**, 381–390.
3 G. R. Helz and R. J. Kleber, Indirect Photoreduction of aqueous chromium(VI), *Environ. Sci. Technol.*, 1992, **26**, 307–312.
4 Z. Zulfadhly, M. D. Mashitah and S. Bhatia, Heavy metals removal in fixed-bed column by the macro fungus Pycnoporus sanguineus, *Environ. Pollut.*, 2001, **112**, 463–470.
5 M. Omraei, H. Esfandian, R. Katal and M. Ghorbani, Study of the removal of Zn(II) from aqueous solution using polypyrrole nanocomposite, *Desalination*, 2011, **271**, 248–256.
6 H. Yuvaraj, M. H. Woo, E. J. Park, Y. T. Jeong and K. T. Lim, Polypyrrole/γ-Fe_2O_3 magnetic nanocomposites synthesized in supercritical fluid, *Eur. Polym. J.*, 2008, **44**, 637–644.
7 B. Saoudi, N. Jammul, M.-L. Abel, M. M. Chehimi and G. Dodin, DNA adsorption onto conducting polypyrrole, *Synth. Met.*, 1997, **87**, 97–103.
8 X. Zhang, R. Bai and Y. W. Tong, Selective adsorption behaviors of proteins on polypyrrole-based adsorbents, *Sep. Purif. Technol.*, 2006, **52**, 161–169.
9 M. Karthikeyan, K. K. Satheeshkumar and K. P. Elango, Removal of fluoride ions from aqueous solution by conducting polypyrrole, *J. Hazard. Mater.*, 2009, **167**, 300–305.
10 S. Zhou, A. Xue, Y. Zhao, Q. Wang, Y. Chen, M. Li and W. Xing, Competitive adsorption of Hg^{2+}, Pb^{2+} and Co^{2+} ions on polyacrylamide/attapulgite, *Desalination*, 2011, **270**, 269–274.
11 X. Zou, J. Pan, H. Ou, X. Wang, W. Guan, C. Li, Y. Yan and Y. Duan, Adsorptive removal of Cr(III) and Fe(III) from aqueous solution by chitosan/attapulgite composites: equilibrium, thermodynamics and kinetics, *Chem. Eng. J.*, 2011, **167**, 112–121.
12 L. Yang, Y. Li, H. Hua, X. Jin, Z. Ye, Y. Ma and S. Zhang, Preparation of novel spherical PVA/ATP composites with macroreticular structure and their adsorption behavior for methylene blue and lead in aqueous solution, *Chem. Eng. J.*, 2011, **173**, 446–455.
13 C. J. Li, B. X. Ma and X. X. Huo, Characterization of graphitization degree in C/C composites(I), *New Carbon Mater.*, 1999, **14**, 19–25.
14 M. Karthikeyan, K. K. Satheesh Kumar and K. P. Elango, Batch sorption studies on the removal of fluoride ions from water using eco-friendly conducting polymer/biopolymer composites, *Desalination*, 2011, **267**, 49–56.
15 Y. Yu, C. Ouyang, Y. Gao, Z. Si, W. Chen, Z. Wang and G. Xue, Synthesis and characterization of carbon nanotube/

polypyrrole core–shell nanocomposites *via in situ* inversemicroemulsion, *J. Polym. Sci., Part A: Polym. Chem.*, 2005, **43**, 6105–6115.

16 A. Maity and S. Sinha Ray, Highly conductive core–shell nanocomposite of poly*N*vinylcarbazole – polypyrrole with multiwall carbon nanotubes, *Macromol. Rapid Commun.*, 2008, **29**, 1582–1587.

17 A. A. Khan and R. P. Singh, Adsorption Thermodynamics of Carbofuran on Sn(VI) Arsenosilicate in H^+, Na^+ and Ca^{2+} Forms, *Colloids Surf.*, 1987, **24**, 33–42.